Nature of the smectic-*A*–smectic-*C* transition of a partially perfluorinated compound

T. Stoebe,[1] L. Reed,[2] M. Veum,[2] and C. C. Huang[2]*
[1]*Department of Chemical Engineering and Materials Science, University of Minnesota, Minneapolis, Minnesota 55455*
[2]*School of Physics and Astronomy, University of Minnesota, Minneapolis, Minnesota 55455*
(Received 9 January 1996)

The smectic-*A*–smectic-*C* phase transition of one partially perfluorinated liquid-crystal compound has been investigated by performing detailed calorimetric studies of both bulk samples and free-standing films. The heat-capacity data from thin free-standing films demonstrate the importance of fluctuations due to reduced dimensionality. Moreover, the data from bulk samples and thick films cannot be adequately described by the customary extended mean-field model. Discussions of other fitting schemes are presented. The free-standing film and bulk data are most consistent with a functional form based on the extended mean-field model but including Gaussian fluctuations. Moreover, the inclusion of Gaussian fluctuation terms adequately accounts for the observed film thickness dependence of smectic-*A*–smectic-*C* heat-capacity anomaly exhibited by this partially perfluorinated compound. [S1063-651X(96)07108-5]

PACS number(s): 64.70.Md, 61.30.−v, 65.90.+i

I. INTRODUCTION

The smectic-*A* (Sm-*A*) and smectic-*C* (Sm-*C*) phases of liquid crystals can be characterized as stacks of two-dimensional (2D) orientationally ordered fluids. The stacks comprise smectic layers and are described by a one-dimensional mass-density wave. In the Sm-*A* (Sm-*C*) phase, the molecular directors are, on average, oriented parallel (at some angle, θ) to the wave vector describing this mass-density wave. The molecular tilt has been established as the primary order parameter discussed with the Sm-*A*–Sm-*C* phase transition. If the constituent molecules are optically active, instead of the Sm-*C* phase, the chiral smectic-*C* (Sm-*C**) phase is observed [1]. Because of the chirality, the Sm-*C** phase exhibits an additional helical structure as the molecular directors of adjacent layers precess around the normal to the layers. Despite this additional order, detailed calorimetric and electro-optical investigations of two chiral liquid-crystal compounds [2,3] have confirmed that the molecular tilt angle remains the primary order parameter associated with the Sm-*A*–Sm-*C** transition [4].

By assuming that the order parameter associated with the Sm-*A*–Sm-*C* transition is of the form $\Psi=\theta\exp(i\phi)$, in 1972, de Gennes [5] asserted that this transition should belong to the three-dimensional (3D) *XY* universality class and might be continuous. The molecular tilt relative to the layer normal is described by θ, and ϕ represents the azimuthal angle of the director. Eight years later, detailed x-ray diffraction studies [6] demonstrated the mean-field-like behavior of this transition. Employing the Ginsburg criterion [7], Safinya *et al.* [6] have argued that the reduced temperature critical region for the Sm-*A*–Sm-*C* transition may be smaller than 10^{-5}. Subsequent high-resolution calorimetric investigations [8] revealed the novelty of this phase transition. It is mean field but is also very near a tricritical point. Based on their heat-capacity data near a Sm-*A*–Sm-*C* transition, Huang and Viner proposed the following extended mean-field model [8] to describe the nature of this transition:

$$G=G_0=at|\Psi|^2+b|\Psi|^4+c|\Psi|^6. \tag{1}$$

Here G_0 is the nonsingular part of the free energy, Ψ is the order parameter, the coefficients a, b, and c are positive for a continuous transition, and $t=(T-T_c)/T_c$ is the reduced temperature. In the vicinity of the transition temperature (T_c), the temperature variation of the heat capacity can be calculated based on this model as

$$C_p=\begin{cases} C_0, & \text{for } T>T_c \\ C_0+AT|T_m-T|^{-1/2}, & \text{for } T<T_c. \end{cases} \tag{2}$$

The nonsingular part of the free energy, G_0, contributes C_0, which can be approximated as linear in reduced temperature (i.e., $C_0=E+Dt$) near T_c. The coefficient $A=a^{3/2}/[2(3c)^{1/2}T_c^{3/2}]$ and the heat capacity would diverge at T_m $[=T_c(1+t_0/3)]$. The important parameter $t_0=b^2/ac$ (equal to the full width at half maximum of the heat-capacity anomaly in reduced temperature) is a dimensionless quantity that characterizes the crossover between the mean-field tricritical region ($b\approx 0$) and the ordinary mean-field regime ($c\approx 0$). To date, many liquid-crystal compounds have yielded the following values: $t_0\approx 10^{-3}$ and $t_G\approx 10^{-5}$. Here the Ginsburg parameter $t_G=k_B^2/[32\pi^2(\Delta C_p)^2\xi_0^6]$. ΔC_p and ξ_0 are the mean-field heat-capacity jump and bare correlation length, respectively. Thus, as these systems approach the Sm-*A*–Sm-*C* transition temperature (T_c), one should observe mean-field-tricritical ($|t|>t_0$) and ordinary mean-field behavior ($t_G<|t|<t_0$) before critical fluctuations become dominant in the immediate vicinity of T_c.

By analyzing twelve different liquid-crystal compounds exhibiting the Sm-*A*–Sm-*C* (or Sm-*C**) transitions. Huang and Lien [9] have found that the nature of this transition is related to the size of the Sm-*A* temperature range. Specifically, the window of the ordinary mean-field region is reduced as the Sm-*A* temperature range (ΔT_A) decreases. Even though none of these twelve compounds displays a

*Electronic address: huang001@maroon.tc.umn.edu

first-order Sm-A–Sm-C (or Sm-C^*) transition, the analysis strongly suggests that compounds with a sufficiently small ΔT_A (less than approximately 6 K [9] would most likely exhibit a first-order Sm-A–Sm-C (or Sm-C^*) transition, as predicted by a coupled mean-field model [10]. It should be noted that the compounds available at that time displayed relatively small transverse polarizations, $P<5$ nC/cm^2, in the Sm-C^* phase.

Subsequent detailed calorimetric and electro-optical studies near the Sm-A–Sm-C^* transition of DOBA-1-MPC (p-decyloxybenzylidene-p'-amino-1-methylpropylcinnamate) were performed [3]. This compound possesses a moderate transverse polarization ($P\approx 20$ nC/cm^2) [11]. Although it exhibits a fairly large Sm-A temperature range ($\Delta T_A\approx 14.5$ K), it was found to exhibit the smallest value of t_0 ($\approx 5.5\times 10^{-4}$) then observed among pure compounds. This transition is therefore extremely close to the mean-field tricritical point. This study provided the first indication of the dependence of the Sm-A–Sm-C^* transition on polarization.

In light of numerous practical applications utilizing ferroelectric liquid crystals [12], many new compounds have been synthesized that exhibit intriguing properties. Examples include compounds with a large transverse polarization ($P>100$ nC/cm^2) [13], novel compounds exhibiting antiferroelectric [14] and twist-grain-boundary phases [15], and partially perfluorinated compounds [16]. To the best of our knowledge, some large transverse polarization compounds were the first to exhibit discontinuous Sm-A-Sm-C^* transitions, despite possessing fairly large Sm-A temperature ranges (greater than 8 K) [13]. This discovery has facilitated an important identification of unique mean-field tricritical behavior in a racemic mixture [17] and several binary mixtures [17] involving compounds with large polarizations. A subsequent mean-field model was put forward [18] to address the effects of the molecular transverse polarization on the nature (continuous or discontinuous) of the Sm-A–Sm-C^* transition. In this paper, we will report that the partial perfluorination of one liquid-crystal molecule also has a dramatic effect on the nature of the Sm-A–Sm-C transition. Furthermore, a model including a contribution due to Gaussian fluctuations has been found to adequately account for our experimental heat-capacity results.

Although the mean-field nature of the Sm-A–Sm-C transition in liquid-crystal compounds has been established by numerous experiments, the theoretical understanding of this behavior remains weak. Based on the measured heat-capacity jump, ΔC_p, and the assumption that the bare correlation length, $\xi_0=(\xi_\perp^2\xi_\parallel)^{1/3}$, is roughly the size of the molecule, the Ginsburg criterion [7] yields $t_G\approx 10^{-5}$. This small value for t_G indicates that the reduced temperature region $|t|<t_G$ in which critical fluctuations are expected to be important is virtually inaccessible in experiments. Since the Sm-C ordering is presumably not driven by long-range interactions and the Sm-A–Sm-C transition is not at or above the upper critical dimensionality ($d_u=4$ for the XY universality class), current theory fails to offer a reasonable explanation for the observed mean-field nature, not to mention the tricritical-like behavior.

According to the symmetry of the order parameter, the Sm-A–Sm-C transition should possess heliumlike behavior. Nonetheless, the quasi-long-range smectic layer order in three dimensions means that the smectic layering is best described by a sinusoidal mass density wave and large fluctuations are possible. Some aspects of the effects of layer undulation on the nature of the Sm-A–hexatic-B (Hex-B) transition [19] were considered by Selinger [20]. It remains extremely important, however, to further investigate the implications of the quasi-long-range (as opposed to truly long-range) nature of the Sm-A order on the molecular tilt order established through the Sm-A–Sm-C transition and on the bond-orientational order established through the Sm-A–Hex-B transition [21]. Meanwhile, any liquid-crystal system exhibiting *critical fluctuations* associated with the Sm-A–Sm-C transition would be of great interest.

Furthermore, it has been argued theoretically and demonstrated by experiment that the mean-field nature of the Sm-A–Sm-C transition possesses another interesting feature. Namely, the Ginsburg parameter t_G may not be the same for different physical quantities. For example, the value of t_G for the ultrasound velocity and attenuation is about 100 times larger than that for the heat capacity [22]. Similar behavior has been reported near the ferroelastic-ferroelectric transition of $Tb_2(MoO_4)_3$ [23]. Nevertheless, identifying and understanding liquid-crystal compounds that display *critical fluctuations* in the heat-capacity data near the Sm-A–Sm-C transition remains an important task. Moreover, the quantitative description and fitting of heat-capacity data is more straightforward than the analysis associated with sound velocity and attenuation.

II. EXPERIMENTAL RESULTS

Employing our bulk [24] and free-standing film calorimeters [25], we have carried out high-resolution heat-capacity measurements near the Sm-A–Sm-C transition of 5-n-decyl-2-(4-n-(perfluoropentyl-metheleneoxy) phenyl) pyrimidine [H10F5MOPP]. The molecular structure is

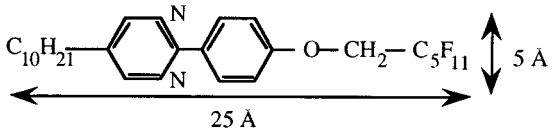

H(10)F(5)MOPP

The transition sequence is isotropic(I) (84 °C) Sm-A (73 °C) Sm-C (47 °C) crystal. This compound possesses a fairly large Sm-A temperature range (about 11 K). The heat-capacity data near the Sm-A–Sm-C transition from our bulk calorimeter are shown in Fig. 1 [26]. The data display a very sharp anomaly (the full width at half maximum (FWHM) is about 2×10^{-4} in reduced temperature), indicating the close proximity of this transition to a mean-field tricritical point. Any thermal hysteresis between cooling and heating runs is less than our experimental resolution of 3 mK and the transition therefore appears to be continuous.

Employing our unique free-standing film calorimeter, we have conducted high-resolution heat-capacity studies on 135-, 80-, 40-, 35-, 30-, 25-, 20-, 16-, and 11-layer films. Most of the data are presented in Figs. 2–5. The 135-, 80-, and 40-layer films exhibit sharp heat-capacity anomalies similar to the bulk data. Significant rounding and broadening of the heat-capacity data becomes increasingly apparent in

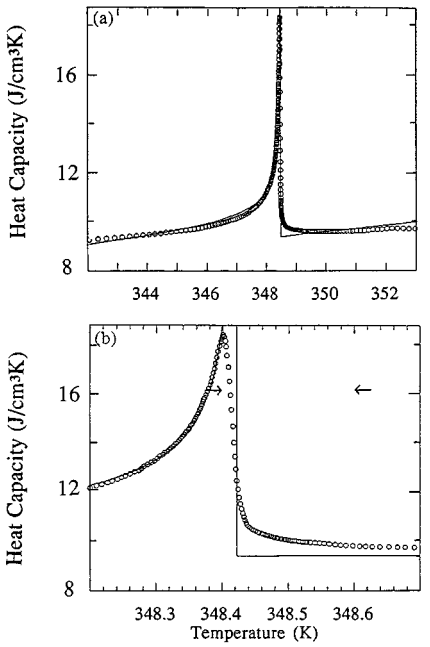

FIG. 1. Temperature dependence of the heat capacity of a bulk H10F5MOPP sample near the Sm-A–Sm-C transition. The solid lines are the best fitting result to Eq. (2). (a) The full temperature range. (b) A more detailed illustration near T_c. The arrows indicate the window of data excluded from the fit.

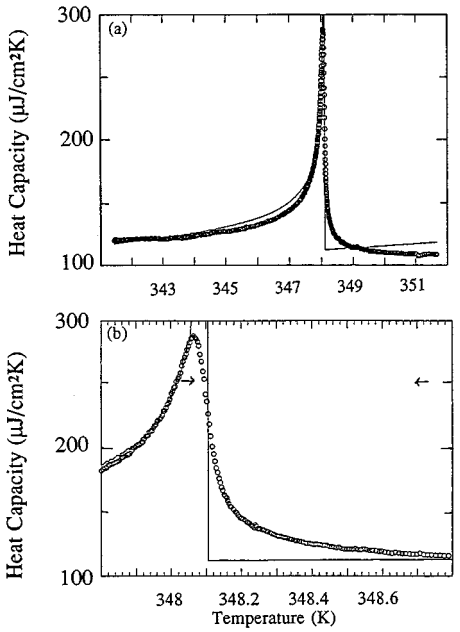

FIG. 3. Heat capacity vs temperature of a 40-layer H10F5MOPP film near the Sm-A–Sm-C transition. The solid lines are the best fitting result to Eq. (2). (a) The full temperature range. (b) A more detailed illustration near T_c. The arrows indicate the excluded temperature window.

the thinner films. In fact, in the case of the 16- and 11-layer films (Fig. 5), the main heat-capacity peak near 348 K is replaced by a broad hump. The observed evolution as a function of film thickness is very different from the data obtained on other liquid-crystal transitions, e.g., Sm-A–Hex-B, [25,27] Sm-A–crystal-B, [28] and Sm-C–Sm-I [29] transitions. The results from the 11-layer film indicate that our experimental resolution must be improved significantly to observe the heat-capacity anomaly associated with still thinner films, in particular 2-layer films.

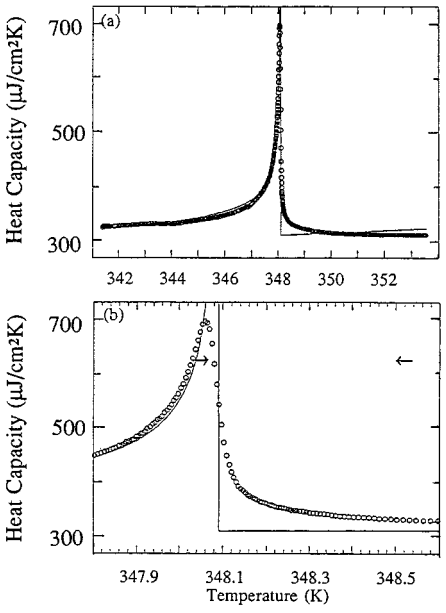

FIG. 2. Temperature variation of the heat capacity from an 80-layer H10F5MOPP film near the Sm-A–Sm-C transition. The solid lines are the best fitting result to Eq. (2). (a) The full temperature range. (b) A more detailed illustration near T_c. The arrows indicate the excluded temperature window.

To quantify the evolution of these heat-capacity data, both t_{FWHM} and $\Delta T_{10-90\%}$ are plotted in Fig. 6 as a function of film thickness. Here t_{FWHM} is the full width at half maximum of the anomaly in reduced temperature and $\Delta T_{10-90\%}$ is the width of the 10–90% heat-capacity jump on the high-temperature side of the anomaly. Both t_{FWHM} and $\Delta T_{10-90\%}$ increase rapidly with decreasing film thickness below 40 layers. Although this may be partially accounted for by finite film thickness rounding, we believe that an enhancement in fluctuations due to reduced dimensionality is

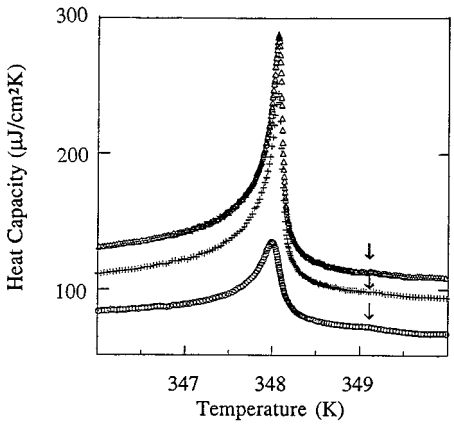

FIG. 4. Temperature dependence of heat capacity of 40-, 35-, and 25-layer H10F5MOPP films near the Sm-A–Sm-C transition. The heat-capacity hump associated with the surface ordering is indicated by arrows.

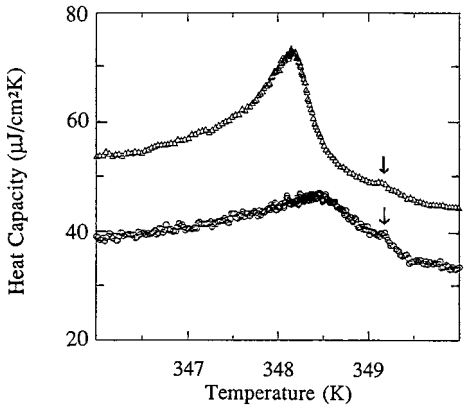

FIG. 5. Heat capacity as a function of temperature for 16- and 11-layer films. The heat-capacity hump associated with the surface ordering is indicated by arrows.

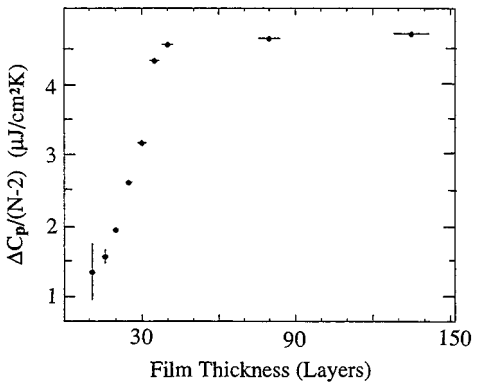

FIG. 7. $\Delta C_p/(N-2)$ vs the layer number (N). Here we assume that the main heat-capacity peak is due to the $N-2$ interior layers (see Ref. [36]).

the major source of the observed trend. It is not clear why this Sm-A–Sm-C transition yields such a distinct dependence on film thickness relative to the other smectic mesophase transitions investigated. However, the distinction may be related to the observation that, unlike the Sm-A–Hex-B, Sm-A–crystal-B, and Sm-C–Sm-I transitions, *both* the Sm-A and Sm-C phases possess purely liquidlike positional and bond-orientational orders within the layers.

It is important to note that a small hump is clearly discernible on the high-temperature side of the main heat-capacity peak of the thinner films (see Figs. 4 and 5). We were, however, unable to detect any other features at temperatures up to (and above) the bulk Sm-A–isotropic transition at which point the film ruptured [30]. We believe that the humps shown in Figs. 4 and 5 signal preferential Sm-C ordering at the surface of the films. This hump may represent the first experimental observation of the heat-capacity anomaly predicted by the Kosterlitz-Thouless theory of 2D defect-mediated transitions [31]. Unfortunately, the signal-to-noise ratio is presently insufficient to resolve this important point. Because polarized optical microscopy failed to reveal characteristic Sm-C director fluctuations, the thin films appear entirely Sm-A at temperatures just above this small hump. Based on these results, it is not possible to determine the number of smectic layers that actually contribute to this surface-induced ordering transition. However, we believe that the initial surface ordering transition would most likely include only the two outermost layers [32]. Such behavior would be consistent with existing experimental results near the Sm-A–Sm-C (or –Sm-C*) transition of other liquid-crystal compounds [33]. Namely, a single surface transition is observed but is apparently not followed by other localized transitions. Unlike other smectic liquid-crystal transitions [25,27–29,34], the Sm-A–Sm-C (or –Sm-C*) transition does not appear to initially progress as a stepwise series of surface-enhanced layer-by-layer transitions [35]. The single surface-enhanced Sm-A–Sm-C* transitions occurs roughly 17 K above the bulk transition in 10-layer DOBAMBC [p-decyloxybenzylidene-p'-amino-(2-methylbutyl)cinnamate] films. Because the apparent surface transition of the 11-layer H10F5MOPP film occurs only about 1 K above the main anomaly, this system seems to be different from DOBAMBC.

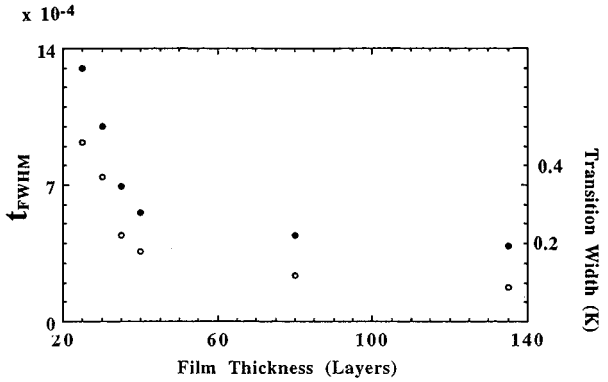

FIG. 6. Plot of transition width ($\Delta T_{10-90\%}$, denoted by open circles) and full width at half maximum in reduced temperature (t_{FWHM}, denoted by solid dots) as a function of film thickness (in units of layers).

The magnitude of the heat-capacity jump (ΔC_p) on the high-temperature side of the anomaly also displays a systematic variation with film thickness. This is illustrated in Fig. 7 where $\Delta C_p/(N-2)$ (normalized to account for the presumed surface ordering) [36] is plotted versus layer number (N). A precipitous drop in $\Delta C_p/(N-2)$ for $N<35$ is consistent with the increasing importance of fluctuations as the film thickness is reduced. This result is also very different from the observed behavior of three other liquid-crystal phase transitions upon reducing film thickness [25,27–29]. We have attempted to account for the unusual heat-capacity data of the free-standing films and bulk samples by applying one distinct modeling scheme.

Two other models [37,38] were considered in our description of the bulk heat-capacity data. The major shortcoming of these two approaches is that there exists no appropriate extension for describing the heat capacity of thin films. Thus we will only present one of them in detail.

III. DATA ANALYSES AND DISCUSSION

To date, the physical properties obtained near the Sm-A–Sm-C (or Sm-C*) transitions of most liquid-crystal compounds have been well described by the customary extended mean-field model [8]. The fitting of our bulk data to Eq. (2)

TABLE I. List of the fitting parameters.

Sample	A ($J/cm^3\,K^{3/2}$)	B ($J/cm^3\,K$)	D ($J/cm^3\,K$)	T_M (K)	T_c (K)	$C_+^{(c)}$ ($J/cm^4\,K$)
bulk[a]	3.88×10^{-3}	9.33	46.75	348.420		
bulk[b]	3.17×10^{-3}	9.15	38.09	348.423	348.416	1.05×10^{5}
	($\mu J/cm^2\,K^{3/2}$)	($\mu J/cm^2\,K$)	($\mu J/cm^2\,K$)	(K)	(K)	($J/cm^3\,K$)
80-layer [a]	0.206	308.62	836	348.090		
80-layer [b]	0.131	294.37	331.46	348.123	348.083	7.22

[a]Fitting to the mean-field expression [Eq. (2)].
[b]Fitting to an expression including contributions from both mean-field and Gaussian fluctuations [Eq. (4)].

with a reasonable excluded temperature region ($348.6>T>348.4$ K, $\Delta T_{ex}=0.2$ K) [39] is included in Fig. 1 as the solid lines. The fitting parameters are listed in Table I. The most striking difference between this fit and previous fits of other Sm-A–Sm-C heat-capacity data to the extended mean-field model is that a large background slope is required. In fact, the slope necessary to provide a good fit for $T<T_c$ is so large that the fit actually crosses the data in the region $T>T_c$. Similar results have been obtained for the 135-, 80-, and 40-layer films (see Figs. 2 and 3). The customary extended mean-field model is, therefore, insufficient to describe both our bulk sample and thick film data.

Motivated by the proximity of this transition to a mean-field tricritical point ($t_0\approx10^{-5}$), we have tried to remedy this discrepancy by including scaling correction terms suggested by Stine and Garland [37]. The expanded heat-capacity expression can be written as

$$C_p=\begin{cases} B_3^+ + D_3 t, & T>T_c \quad (3a)\\ B_3^- + D_3 t + A_3|t|^{-1/2}(1+D_{31}|t|+D_{32}|t|^{3/2}), & T<T_c\,. \quad (3b)\end{cases}$$

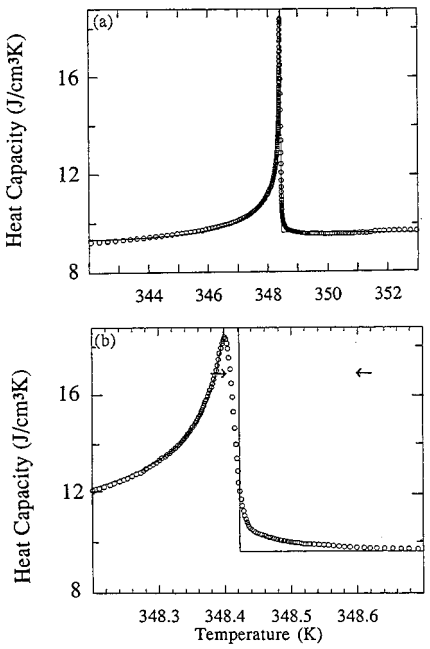

FIG. 8. The heat-capacity data from the bulk sample. The solid lines are the fitting result to Eq. (3). (a) The full temperature window. (b) A detailed illustration near T_c. The arrows indicate the excluded temperature region ($\Delta T_{ex}=0.2$ K).

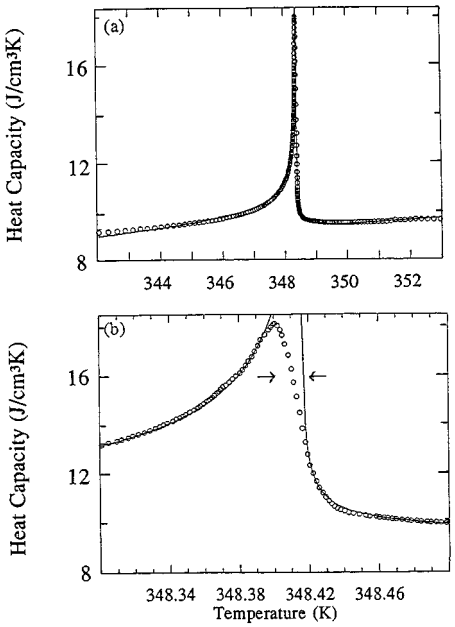

FIG. 9. The heat-capacity data from the bulk sample. The solid lines are the fitting result to Eq. (4). (a) The full temperature window. (b) A detailed illustration near T_c. The arrows indicate the excluded temperature region ($\Delta T_{ex}=0.02$ K).

To ensure that the divergent heat capacity is the most singular term near the transition, we take $B_3^+ = B_3^-$. The existence of the correction to the scaling term proportional to $|t|^{3/2}$ allows the effective background slope s to differ above ($s = D_3$) and below ($s = D_3 - A_3 D_{32}$) the transition temperature. This feature obviously improves the deficiency of the previous extended mean-field fitting. A difference in slopes for $T > T_c$ and $T < T_c$ suggests odd singular behavior in the linearly dependent part of the heat capacity. If the slopes are forced to be equal ($D_{32} = 0$), this fitting scheme results in no significant improvement over the results obtained using the customary extended mean-field model. Allowing D_{32} to vary, nonlinear least-squares fitting to Eq. (3) yields the solid line as shown in Fig. 8 with an excluded region $348.4 < T < 348.6$ K ($\Delta T_{ex} = 0.2$ K). The values of the fitting parameters are $A_3 = 3.95 \times 10^{-3}$ J/cm^3 K, $B_3 = 9.59$ J/cm^3 K, $D_3 = 1.03$ J/cm^3 K, $D_{31} = -2.00 \times 10^2$, $D_{32} = 8.60 \times 10^2$, and $T_c = 348.422$ K. Although this fitting is satisfactory, it requires two additional fitting parameters (D_{31} and D_{32}) and a large excluded fitting region ($\Delta T_{ex} = 0.2$ K). Moreover, two other sets of heat-capacity data near the Sm-A–Sm-C mean-field tricritical point did not require additional scaling correction terms to produce satisfactory fits [17]. The improvement in fitting by this model may therefore be fairly incidental and due primarily to the addition of the $|t|^{3/2}$ scaling correction term for $T < T_c$. Furthermore, to the best of our knowledge, this model cannot be applied to our film data as no extension to systems of finite thickness has been developed.

It is appropriate to stress that two other liquid-crystal compounds [17] exhibiting mean-field tricritical behavior were well described by the extended mean-field model [Eqs. (1) and (2)] without the expansions associated with Eq. (3). In light of the experimental data suggesting the importance of fluctuations to the heat-capacity anomalies of the thin films, it is reasonable to attempt to further investigate the extended mean-field model by including terms characteristic of Gaussian fluctuations. A heat-capacity expression has been developed based on the extended mean-field model to also account for Gaussian fluctuations in systems of finite thickness (d) and bulk ($d = \infty$) [40,41] samples:

$$C_p = \begin{cases} C_0 + (C_+/d)(T/T_c)^2 \xi^2 [1 + (d/\xi)\coth(d/\xi)], & T > T_c \quad (4a) \\ C_0 + AT|T_m - T|^{-1/2} + 2(C_-/d)(T/T_c)^2 \xi'^2 [1 + (d/\xi')\coth(d/\xi')], & T < T_c . \quad (4b) \end{cases}$$

Here $\xi' = 2^{-1/2}\xi = 2^{-1/2}\xi_0 |t|^{-1/2}$ and ξ_0 is the bare correlation length for the fluctuations. The best fitting results were obtained for very reasonable values of the bare correlation length (0.25 layer $< \xi_0 < 0.55$ layer). To reduce the number of fitting parameters, ξ_0 was thereafter fixed at $\xi_0 = 0.4$ layer. Because Fig. 7 suggests that the heat-capacity anomalies for films thicker than 35 layers are primarily bulklike, we were able to further reduce the number of fitting parameters by invoking the 3D XY scaling relation between C_- and C_+ ($C_- = 2^{1/2} C_+$). Under these circumstances, C_+ and T_c are

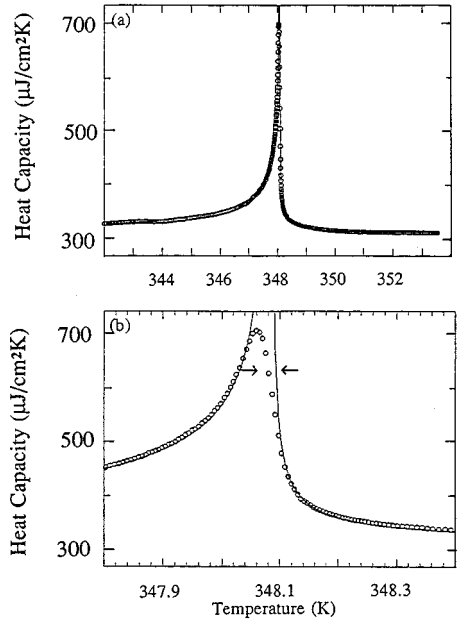

FIG. 10. The heat-capacity data from an 80-layer film. The solid lines are the fitting result to Eq. (4). (a) The full temperature window. (b) A detailed illustration near T_c. The arrows indicate the excluded temperature window ($\Delta T_{ex} = 0.04$ K).

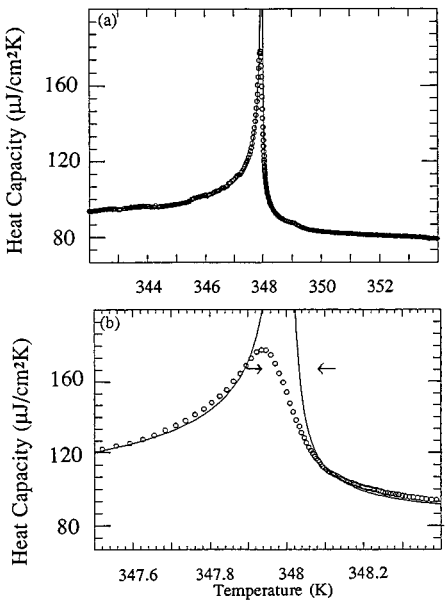

FIG. 11. The heat-capacity data from a 30-layer film. The solid lines are the fitting result to Eq. (4). (a) The full temperature window. (b) A detailed illustration near T_c. The arrows indicate the excluded temperature region ($\Delta T_{ex} = 0.13$ K).

the only two additional fitting parameters associated with the inclusion of Gaussian fluctuations in the analysis. The results of this approach are displayed as solid lines in Figs. 9 and 10 for the bulk sample and 80-layer film, respectively. These fits are clearly superior to those presented in Figs. 1 and 2. The parameters are listed in Table I. It is important to note that, besides the superior fitting, this approach requires a significantly smaller region of excluded temperature. To the best of our knowledge, this is the first case in which the addition of Gaussian fluctuation terms provide a significantly better description of the Sm-A–Sm-C transition and yield seemingly reasonable values for the fitting parameters.

Equation (4) was also used to fit the heat-capacity data from 35-, 30-, and 25-layer films. Meaningful fits could be obtained only by dramatically increasing the excluded temperature window from 100 mK for the 35-layer-film data to 200 mK for the 25-layer-film data. The results for the 30-layer film data are plotted in Fig. 11. Aside from the large excluded temperature window and inability to follow the small hump resumably associated with preferential surface ordering, the fitting results are fairly reasonable. We know of no existing fitting expression that could account for the combined finite-size and preferential surface ordering effects apparently displayed by our data. An observed systematic variation of the fitting coefficients with film thickness could guide the theoretical analysis and would therefore be of considerable interest. The fitting results obtained yield the following values for C_+/A (in $K^{1/2}$): 62.9, 55.0, 38.2, 51.3, 50.5, and 40.2, respectively, for the 135-, 80-, 40-, 35-, 30-, and 25-layer films. Because this ratio provides some indication of the relative strength of the fluctuation and mean-field contributions to the heat capacity, it might be expected to increase with decreasing film thickness. The apparent lack of any such dependence does not support our interpretation of the data. However, the significantly increased excluded temperature windows necessary for thinner films is strongly suggestive of a deficiency of the model. A more complete theoretical description is clearly necessary to better account for our data.

A recent x-ray study [42] of free-standing films of a perfluorinated compound similar to H10F5MOPP yielded the smectic compressional elastic modulus $B \approx 10^9$ erg/cm. This value is roughly 100 times larger than the value typically exhibited by simple alkyl terminated liquid-crystal compounds [43]. This is consistent with the fact that the perfluoropentyl chain is bulkier and more rigid than a corresponding alkyl chain. Moreover, we believe that the observed layer-by-layer thinning transition above the Sm-A–isotropic transition of H10F5MOPP [30] is related to similarly atypical elastic properties associated with the partial perfluorination. This difference in elastic constants provides a plausible argument for the increased probability of observing critical fluctuations near the Sm-A–Sm-C transition of these compounds.

The Ginsburg parameter t_G for the Sm-A–Sm-C transition can also be written as [44]

$$t_G = [k_B T b/(\pi C_\perp C_\parallel^{1/2})]^2/(2a). \tag{5}$$

Here a and b are the coefficients defined in Eq. (1) and $C_\perp$ ($C_\parallel$) is the elastic constant perpendicular (parallel) to the smectic layer normal. In addition to Eq. (1), the following terms are also important in describing the Sm-A-Sm-C transition:

$$G_c = \lambda |\Psi|^2 \Delta + B\Delta^2. \tag{6}$$

The coupling between tilt ($|\Psi|$) and layer dilatation (Δ) is described by the first term with a coupling constant λ. The second term accounts for the layer compressional elastic energy. Minimizing with respect to Δ yields the renormalized coefficient:

$$b = b_0 - \lambda^2/4B. \tag{7}$$

Thus a large value of B tends to diminish the reduction of b, thereby increasing the parameter t_G. By employing this argument [44], partially perfluorinated compounds (possessing a large value for B) are more likely candidates than ordinary alkyl compounds to reveal fluctuation effects in the heat capacity near the Sm-A–Sm-C transition. This point is obviously consistent with our experimental data and fitting results.

In conclusion, we have shown the customary extended mean-field model to be insufficient to describe the measured heat-capacity anomalies associated with the Sm-A–Sm-C transition in bulk samples and free-standing films of the partially perfluorinated H10F5MOPP compound. Two different models have been explored to account for the bulk data and fairly reasonable fits were obtained. Unfortunately the theory has not yet been developed to apply either of these models to systems of finite thickness. The bulk and moderately thick free-standing heat-capacity data could, however be successfully fit by a model including the effects of Gaussian fluctuations. Although the characterization of these intriguing partially fluorinated compounds is far from complete, a number of interesting and unusual physical phenomena have already been revealed [16,30,42,45]. Further studies on this remarkable group of liquid-crystal compounds are in progress.

Recently, critical behavior has been reported near the Sm-A–Sm-C^*_α transition of an antiferroelectric liquid-crystal compound [46] and the Sm-A-Sm-C transition of the racemic mixture [46]. It is important to investigate the origin of critical fluctuations that should shed important light on the mean-field nature of the Sm-A–Sm-C transition found in customary liquid-crystal compounds.

ACKNOWLEDGMENTS

We are grateful to Professor C. W. Garland, Professor A. M. Goldman, Professor D. Nelson, Professor T. Lubensky, Professor J. Prost, and Professor W. H. de Jeu for valuable discussions and would like to thank Dr. K. A. Epstein and Dr. M. D. Radcliffe (3M Corporation, St. Paul, MN) for providing the partially perfluorinated samples. This work was supported in part by the National Science Foundation, Solid State Chemistry Program, Grant No. DMR-93-00781.

[1] R. B. Meyer, L. Liebert, L. Strzelecki, and P. Keller, J. Phys. (Paris), Lett. **36**, 69 (1975).
[2] C. C. Huang and S. Dumrongrattana, Phys. Rev. A **34**, 5020 (1986).
[3] C. C. Huang, S. Dumrongrattana, G. Nounesis, J. J. Stofko, Jr., and P. A. Arimilli, Phys. Rev. A **35**, 1460 (1987).
[4] R. B. Meyer, Mol. Cryst. Liq. Cryst. **40**, 33 (1977).
[5] P. G. de Gennes, Mol. Cryst. Liq. Cryst. **21**, 49 (1973).
[6] C. R. Safinya, M. Kaplan, J. Als-Nielsen, R. J. Birgeneau, D. Davidov, J. D. Litster, D. L. Johnson, and M. Neubert, Phys. Rev. B **21**, 4149 (1980).
[7] V. L. Ginsburg, Fiz. Tverd Tela (Leningrad) **2**, 2031 (1960) [Sov. Phys. Solid State **2**, 1824 (1960)].
[8] C. C. Huang and J. M. Viner, Phys. Rev. A **25**, 3385 (1982).
[9] C. C. Huang and S. C. Lien, Phys. Rev. A **31**, 2621 (1985).
[10] C. C. Huang, Solid State Commun. **43**, 883 (1982).
[11] K. Yoshino, M. Ozaki, T. Sakurai, K. Sakamoto, and M. Honma, Jpn. J. Appl. Phys. **23**, L175 (1984).
[12] N. A. Clark and S. T. Lagerwall, Appl. Phys. Lett. **36**, 899 (1980).
[13] Ch. Bahr and G. Heppke, Mol. Cryst. Liq. Cryst. Lett. **4**, 31 (1986).
[14] A. D. L. Chandani, E. Gorecka, Y. Ouchi, H. Takezoe, and A. Fukuda, Jpn. J. Appl. Phys. **28**, L1265 (1989).
[15] J. W. Goodby, M. A. Waugh, S. M. Stein, E. Chin, R. Pindak, and J. S. Patel, J. Am. Chem. Soc. **111**, 8119 (1989).
[16] E. P. Janulis, D. W. Osten, M. D. Radcliffe, J. C. Novack, M. Tristani-Kendra, K. A. Epstein, M. Keyes, G. C. Johnson, P. M. Savu, and T. D. Spawn, SPIE Int. Soc. Opt. Eng. **1665**, 143 (1992); T. Doi, S. Takenaka, S. Kusabayashi, Y. Nishihata, and H. Terauchi, Mol. Cryst. Liq. Cryst. **204**, 9 (1991).
[17] H. Y. Liu, C. C. Huang, Ch. Bahr, and G. Heppke, Phys. Rev. Lett. **61**, 345 (1988); R. Shashidhar, B. R. Ratna, G. G. Nair, S. K. Prasad, Ch. Bahr, and G. Heppke, *ibid.* **61**, 547 (1988); T. Chan, Ch. Bahr, G. Heppke, and C. W. Garland, Liq. Cryst. **13**, 667 (1993). The mean-field heat-capacity expression at a tricritical point ($b=0$) has been proven to provide an excellent fit to the measured heat-capacity data thought to be in the immediate vicinity of a tricritical point.
[18] H. Y. Liu, C. C. Huang, T. Min, M. D. Wand, D. M. Walba, N. A. Clark, Ch. Bahr, and G. Heppke, Phys. Rev. A **40**, 6759 (1989).
[19] According to the structure information, the Sm-A–Hex-B transition should belong to the XY universality class. To date, all the experimental results fails to show the expected criticality in both bulk samples and extremely thin films.
[20] J. V. Selinger, J. Phys. (Paris) **49**, 1387 (1988).
[21] D. R. Nelson (private communication).
[22] D. Collin, S. Moyses, M. E. Neubert, and P. Martinoty, Phys. Rev. Lett. **73**, 983 (1994); L. Benguigui and P. Martinoty, *ibid.* **63**, 774 (1989).
[23] W. Yao, H. Z. Cummins, and R. H. Bruce, Phys. Rev. B **24**, 424 (1981); A. Fouskova, J. Phys. Soc. Jpn. **27**, 1699 (1969).
[24] J. M. Viner, D. Lamey, C. C. Huang, R. Pindak, and J. W. Goodby, Phys. Rev. A **28**, 2433 (1983).
[25] R. Geer, T. Stoebe, and C. C. Huang, Phys. Rev. E **48**, 408 (1993).
[26] An error was found in previously calculating the units of the measured heat-capacity data [39]. For some unknown reasons, the measured heat capacity of this perfluorinated compound is about twice that of the ordinary liquid-crystal compounds.
[27] A. J. Jin, M. Veum, T. Stoebe, C. F. Chou, J. T. Ho, S. W. Hui, V. Surendranath, and C. C. Huang, Phys. Rev. Lett. **74**, 4863 (1995).
[28] A. J. Jin, T. Stoebe, and C. C. Huang, Phys. Rev. E **49**, R4791 (1994).
[29] T. Stoebe and C. C. Huang, Phys. Rev. E **50**, R32 (1994).
[30] T. Stoebe, P. Mach, and C. C. Huang, Phys. Rev. Lett. **73**, 1384 (1994).
[31] A. N. Berker and D. R. Nelson, Phys. Rev. B **19**, 2488 (1979); S. Solla and E. K. Riedel, *ibid.* **23**, 6008 (1981).
[32] Even though the anomaly from a two-layer film cannot presently be detected, the surface-enhanced ordering transition presumably due to only the two outermost layers of thicker films can still be resolved because of our calorimeter's film thickness dependent signal-to-noise (S/N) ratio. Films of moderate thickness (≈ 20 layers) generally provide the highest quality data. We have determined that S/N must be improved by at least a factor of five before the heat-capacity anomaly associated with the Sm-A–Sm-C transition of two-layer H10F5MOPP films can be convincingly resolved. Several possible approaches are currently being evaluated.
[33] S. Heinekamp, R. A. Pelcovits, E. Fontes, E. Y. Chen, R. Pindak, and R. B. Meyer, Phys. Rev. Lett. **52**, 1017 (1984); S. M. Amador and P. S. Pershan, Phys. Rev. A **41**, 4326 (1990); Ch. Bahr and D. Fliegner, *ibid.* **46**, 7657 (1992).
[34] B. D. Swanson, H. Stragier, D. J. Tweet, and L. B. Sorensen, Phys. Rev. Lett. **62**, 909 (1989); B. D. Swanson and L. B. Sorensen, *ibid.* **75**, 3293 (1995).
[35] Surface ordering has been identified in various other systems, e.g., M. B. Feller, W. Chen, and Y. R. Shen, Phys. Rev. A **43**, 6778 (1991); X. Z. Wu, B. M. Ocko, E. B. Sirota, S. K. Sinha, M. Deutsch, B. H. Cao, and M. W. Kim, Science **261**, 1018 (1993); M. N. G. de Mul and J. A. Mann, Jr., Langmuir **10**, 2311 (1994), and references found therein.
[36] Assuming that the small heat-capacity humps are due to thicker ''surface layers,'' we have tried to plot $\Delta C_p/(N-n)$ versus N. For $n>2$, an up turn in such a plot is identified for thinner films. Thus we conclude that only two outermost surface layers contribute to the small heat-capacity humps.
[37] K. J. Stine and C. W. Garland, Phys. Rev. A **39**, 3148 (1989).
[38] E. E. Gorodetskii and V. M. Zaprudskii, Zh. Éksp. Teor. Fiz. **72**, 2299 (1977) [Sov. Phys. JETP **45**, 1209 (1977)].
[39] L. Reed, T. Stoebe, and C. C. Huang, Phys. Rev. E **52**, R2157 (1995).
[40] N. A. H. K. Rao and A. M. Goldman, J. Low Temp. Phys. **42**, 253 (1981).
[41] S. K. Ma, *Modern Theory of Critical Behavior* (Benjamin, Reading, MA, 1976).
[42] J. D. Shindler, E. A. L. Mol, A. Shalaginov, and W. H. de Jeu, Phys. Rev. Lett. **74**, 722 (1995).
[43] M. Benzekri, J. P. Marcerou, H. T. Nguyen, and J. C. Rouillon, Phys. Rev. B **41**, 9032 (1990).
[44] P. G. de Gennes and J. Prost, *The Physics of Liquid Crystals*, 2nd ed. (Clarendon Press, Oxford, 1993), p. 530.
[45] T. Stoebe, P. Mach, S. Grantz, and C. C. Huang, Phys. Rev. E **53**, 1662 (1996).
[46] K. Ema, J. Watanabe, A. Takagi, and H. Yao, Phys. Rev. E **52**, 1216 (1995); K. Ema, A. Takagi, and H. Yao, *ibid.* (to be published).